Journal of Power Sources 196 (2011) 7924–7930

Contents lists available at ScienceDirect

Journal of Power Sources

journal homepage: www.elsevier.com/locate/jpowsour

Solvent processible, high-performance partially fluorinated copoly (arylene ether) alkaline ionomers for alkaline electrodes

Junfeng Zhou, Murat Ünlü, Irene Anestis-Richard, Hyea Kim, Paul A. Kohl*

Chemical and Biomolecular Engineering, Georgia Institute of Technology, Atlanta, GA 30332-0100, USA

ARTICLE INFO

Article history:
Received 8 March 2011
Received in revised form 5 May 2011
Accepted 12 May 2011
Available online 19 May 2011

Keywords:
Alkaline ionomers
Alkaline electrodes
Fuel cells
Water uptake
Ionic conductivity

ABSTRACT

A solvent processable, low water uptake, partially fluorinated copoly(arylene ether) functionalized with pendant quaternary ammonium groups (QAPAE) was synthesized and uses as the ionomer in alkaline electrodes on fuel cells. The quaternized polymers containing fluorinated biphenyl groups were synthesized via chloromethylation of copoly(arylene ether) followed by amination with trimethylamine. The resulting ionomers were very soluble in polar, aprotic solvents. Highly aminated ionomers had conductivities approaching 10 mS cm^{-1} at room temperature. Compared to previous ionomers based on quaternized poly(arylene ether sulfone) (QAPSF) with similar ion exchange capacity (IEC), the water uptake of QAPAE was significantly less due to the hydrophobic octafluoro-biphenyl groups in the backbone. The performance of the fuel cell electrodes made with the QAPAE ionomers was evaluated as the cathode on a hybrid AEM/PEM fuel cell. The QAPAE alkaline ionomer electrode with IEC = 1.22 meq g^{-1} had superior performance to the electrodes prepared with QAPSF, IEC = 1.21 meq g^{-1} at 25 and 60 °C in a H_2/O_2 fuel cell. The peak power densities at 60 °C were 315 mW cm^{-2} for QAPAE electrodes and 215 mW cm^{-2} for QAPSF electrodes.

1. Introduction

Efficient energy conversion devices are needed meet the ever-increasing energy need and help mitigate global climate change concerns. Efficient and affordable devices include photovoltaic cells, fuel cells, and batteries [1–4]. The electrolytes play a critical role in the advancement of these energy conversion devices. In particular, polymer electrolytes offer fabrication flexibility, improved mechanical strength, and safe-operation compared to liquid and gel electrolytes [1,5]. High ionic conductivity is an essential feature of the polymeric electrolytes, although the specific values depend on the current density, overall potential difference between the electrodes, and device application [6]. In addition, the mechanical properties and chemical stability are important for long life.

Proton conducting polymer electrolytes are highly developed and often used for hydrogen and methanol fuel cells [7]. However, the low pH in proton exchange membranes (PEM) results in poor reaction kinetics and requires noble metal catalysts, which increase the cost. Recently anion exchange membranes (AEMs) have attracted attention because they can potentially address many shortcomings of PEM fuel cells [8]. AEM fuel cells offer fast electrokinetics mitigating the need for platinum-based catalysts and can lower the degree of fuel crossover in part due to the opposite direction of electro-osmotic drag from PEM cells. Additionally, novel AEM/PEM hybrid design enables fuel cell operation without external humidification [9]. However, the cell performance obtained for AEM or AEM/PEM hybrid fuel cells are currently modest compared to PEM fuel cells. This low performance is generally associated with the less-mature and inferior properties of anion exchange ionomer used to construct the electrode. Our recent studies have shown that excessive water uptake in the electrode catalyst layer was largely responsible for the loss of electrode performances in the alkaline AEM electrodes [10]. Excessive water swelling can flood the free volume within the electrode blocking the catalytic sites, and hindering gas transport.

Water management issues in alkaline AEM electrodes are more pronounced than in PEM-based electrodes [11,12]. Nafion has high ionic conductivity (ca. 80 mS cm^{-1}) and low water uptake (30%) due to its perfluorinated backbone. Nafion can also be solubilized in alcohol. These same attributes have not yet been realized in anion conducting polymers. Anionic conducting polymers have been prepared by a variety of aromatic backbone structures using chloromethylation or bromination of the backbone followed by quaternization with trimethylamine. Common polyaromatic backbones include poly(phthalazinon ether sulfone ketone), poly(phenylene), poly(sulfone ether) [13–20]. Other anionic conducting polymers have been synthesized of quaternization of aliphatic polymers containing vinylbenzyl chloride [21,22]

* Corresponding author.
E-mail address: kohl@gatech.edu (P.A. Kohl).

0378-7753/$ – see front matter © 2011 Elsevier B.V. All rights reserved.
doi:10.1016/j.jpowsour.2011.05.024

In general, these anion exchange materials have lower conductivity and higher water uptake than Nafion. Adequate ionic conductivity was obtained at the expense of high water uptake. Thus, the challenge for ionomers needed in high-performance AEM electrodes lies in maintaining good ion conductivity but without excessive swelling.

One strategy to achieve high conductivity without excessive water swelling is to use partial or complete fluorination of the polymer backbone since the hydrophobic backbone structure will lower the tendency to absorb excessive amounts of water. There have been few reports about the synthesis of partially or completely fluorinated anionic exchange polymers. Varcoe and co-workers reported a series of anion exchange materials synthesized by radiation grafting of vinylbenzyl chloride onto partially or completely fluorinated polymers such as poly(ethylene-co-tetrafluoroethylene) (ETFE), poly-(tetrafluoroethylene-co-hexafluoropropylene) (FEP), or poly-(vinylidene fluoride) (PVDF) [23–25]. These polymer electrolytes were used, as the membrane in fuel cells but their use as an ionomer in the preparation of electrodes was not possible because they could not be solubilized. Solubility in appropriate solvents is essential to the construction of anionic electrodes.

Consequently, our approach has been to develop a solvent-processable, hydrophobic ionomer for AEM electrode applications. We have used fluorinated aromatic monomers to synthesize novel, partially fluorinated copoly(arylene ether) functionalized with pendant quaternary ammonium groups. These ionomers can offer many advantages over all hydrocarbon ones due to its unique features. The presence of partially fluorinated units in the main-chain gives the polymer a hydrophobic nature, excellent mechanical strength, and good thermal and chemical stability. The presence of ether groups provides flexibility, facilitating easy processing.

In this study, a series of novel partially fluorinated copoly(arylene ether) functionalized with pendant quaternary ammonium groups were synthesized through polycondensation, chloromethylation, and amination reactions. Hydroxide conductivity and water uptake of the anionic conductors were evaluated. The ionomers were used as the cathode in a PEM-based anode/membrane assembly.

2. Experimental

2.1. Materials

2-Phenylhydroquinone (PHQ) (Aldrich), decafluorobiphenyl (DFBP) (Aldrich), 1,1,2,2-tetrachloroethane (Alfa Aesar), toluene (Alfa Aesar), chloromethyl methyl ether (Aldrich), tin(IV) chloride (Alfa Aesar), and trimethylamine (Alfa Aesar) were used as-received. Potassium carbonate (Aldrich) was dried at 120 °C for 24 h before polymerization. Other chemicals were obtained as reagent grade and used as-received.

2.2. Polymerization of poly(arylene ether)s

[26] In a typical PAE reaction, a 250 mL three-necked round-bottomed flask equipped with a magnetic stirring bar, a N_2 inlet, and an addition funnel, was charged with PHQ (0.03 mol, 5.5863 g), DFBP (0.03 mol, 10.0233 g), potassium carbonate (0.066 mol, 4.8024 g), toluene (45 mL) and DMAc (45 mL). The mixture was stirred at room temperature for 20 min and then heated at 130 °C for 12 h under N_2 atmosphere. After reaction, the solution was poured dropwise into deionized water (2 L) and a white product precipitated from solution. After washing with hot, deionized water and ethanol several times, the polymer, denoted PAE, was dried under vacuum at 60 °C for 15 h.

2.3. Chloromethylation of poly(arylene ether)s

A typical procedure for the chloromethylation of the poly(arylene ether)s is as follows. The chloromethylation reaction was performed in a glass flask heated in an oil bath and equipped with a magnetic stirring bar, a N_2 inlet and a reflux condenser. PAE (3.0011 g) was dissolved in 1,1,2,2-tetrachloroethane (50,000 g, 31.48 mL) solvent, then a mixture of chloromethyl methyl ether (0.0625 mol, 5.0319 g) and $SnCl_4$ (0.9635 mmol, 0.2505 g) was slowly added to the above solution. The reaction was heated to 60 °C for several days. After cooling to room temperature, the mixture was poured into ethanol (1 L). The precipitate was collected by filtration, dried under vacuum, dissolved in 20 mL THF, and reprecipitated into 1 L ethanol to remove unreacted materials and solvent. The polymer precipitate, CMPAE, was collected by filtration and dried under vaccum to yield an off-white solid.

2.4. Amination of CMPAE

The following represents a typical procedure for the amination of CMPAE. The CMPAE powder was added to a 45% (w w^{-1}) solution of trimethylamine in water and the mixture was stirred for 48 h at room temperature. During the reaction, CMPAE with a high degree of chloromethylation (DC) would gradually dissolve in the solution, whereas CMPAE with low DC remained as a powder. After the reaction, the mixture was poured into an evaporating dish to dry the polymer, QAPAE, at room temperature in order to remove unreacted trimethylamine and water.

2.5. Preparation of membranes

QAPAE was dissolved in dimethylformamide (DMF) to make a 5.0 wt% solution. The solution was filtered with a 0.45 μm Teflon syringe filter to remove small particles and poured onto Telfon plates, and dried at 60 °C under a nitrogen purge for 12 h. Alkaline membranes (ca. 70 μm thick) were synthesized and stored in the chloride form. They were converted to the hydroxide form immediately prior to use. Conversion from the chloride form to the hydroxide form was performed as follows. The as-cast membrane in the chloride form was soaked in an aqueous sodium hydroxide solution (0.1 M, at least 10 times excess) for 0.5 h with four changes of NaOH during this period to ensure complete ion exchange. The resulting membrane was then soaked in water for 1 h with at least two changes of water to remove any residual sodium hydroxide.

2.6. Preparation of membrane electrode assembly

The alkaline AEM electrodes were characterized on a semi-hybrid membrane electrode assembly (MEA), as described previously [27]. Hybrid MEAs include one conventional PEM based electrode as the anode and an alkaline AEM electrode as the cathode on a Nafion core membrane. All the PEM-based electrodes in the hybrid MEAs were identical while two types of ionomers were used in the AEM electrodes.

The PEM electrodes were made by a conventional thin-film method consisting of painting a catalyst ink onto carbon paper. The ink was prepared by mixing a Nafion solution (5% by weight), platinum catalyst (20% Pt by weight on carbon, E-TEK), isopropyl alcohol (IPA), and water. The ink was sonicated for 15 min and then cast onto Toray carbon paper (TGPH-090) and dried at room temperature. The ionomer loading was 0.5 mg cm^{-2}.

The ionomers used for the AEM electrodes were (i) quaternized poly(arylene ether sulfone), as described previously [28], and (ii) partially fluorinated and quaternized copoly(arylene ether) synthesized in this study. The alkaline ionomers were used as a 1.0 wt% solution in DMF.

The AEM electrodes were fabricated by casting the anion exchange materials onto a prefabricated catalyst layer (Electrochem). The prefabricated Pt catalyst layers comprised of Teflon binder (with a proprietary amount) but no ionomer. The ionomer (0.5% by weight) in DMF: methanol (1:1 weight ratio) solvent mixture was sprayed on the catalyst surface. The loading of the anion conducting materials was 0.6 mg cm^{-2}. After drying at room temperature, the AEM electrodes were immersed in aqueous 0.5 M KOH to exchange OH^- for Cl^- counter ion in the ionomer.

The catalyst loadings were 0.5 mg cm^{-2} Pt for all the electrodes. All electrodes had a geometric surface area of 2.0 cm^2. Once both the PEM and AEM electrodes were dry, 100 μL of Nafion® (5% suspension): IPA mixture (1:2 by volume) was sprayed onto the AEM and PEM electrodes. The hybrid MEAs were assembled in two steps. In the first step, the PEM electrode was pressed onto Nafion® 212 at 2 MPa gauge pressure and 135 °C temperature for 3 min. In the second step, the AEM electrode was pressed onto the PEM half-cell assembly at 2 MPa and 50 °C for 3 min.

The fuel cell test procedure was performed as previously reported. The fuel cell hardware assembly (Fuel Cell Technologies) consisted of a pair of Poco graphite blocks with a single-serpentine flow pattern. All MEAs were preconditioned by operating at steady state at 600 mV discharge voltage for 24 h before performing current–voltage (*I–V*) polarization experiments. Electrochemical measurements were performed using Arbin BT2000 potentiostat. All fuel cell tests were conducted at ambient pressure.

2.7. Characterization

The ^{1}H-NMR spectra of the synthesized polymers were recorded for structural characterization. The data were collected with a Model DMX400 spectrometer using deutrated chloroform ($CDCl_3$) as the solvent. Thermogravimetry analysis (TGA) was carried out in flowing nitrogen (60 cm^3 min^{-1}) using a TA Q50 thermal analyzer. Samples were heated from ambient temperature to 800 °C at a heating rate of 1.0 °C min^{-1}.

The ion exchange capacity of these membranes was measured using the classical titration method [17,18]. The membranes were immersed in a large volume of 0.1 M NaOH solution to convert them from the chloride form to the hydroxide form. They were then rinsed with deionized water to remove excess NaOH. The hydroxide was neutralized by immersing the samples in 10 mL of 0.01 M HCl solution for 24 h. The IEC was determined by titration of the HCl solution to measure the amount of acid neutralized by the hydroxide. The IEC was obtained from Eq. (1).

$$\mathrm{IEC(meq\,g^{-1})} = \frac{(\mathrm{M}_o - \mathrm{M}_e)}{\mathrm{m}_d} \quad (1)$$

where M_o is the milliequivalents (meq) of HCl measured before membrane neutralization, M_e is the meq of HCl measured after neutralization, and m_d is the mass of the dried membrane.

The water uptake of the membranes was evaluated by first drying the films in a desiccator over anhydrous calcium chloride at ambient temperature until a constant dry weight (W_d) was obtained [17]. The dry membranes were immersed in deionized water at different temperatures for 24 h. The surface water was swabbed away with tissue paper before weighing. The weight was measured several times until a constant weight (W_w) was achieved. The water uptake of membranes was calculated using Eq. (2).

$$\mathrm{Water\ uptake(\%)} = \left[\frac{(\mathrm{W}_w - \mathrm{W}_d)}{\mathrm{W}_d}\right] \times 100\% \quad (2)$$

The in-plane hydroxide conductivity of the samples was measured by four probe electrochemical impedance spectroscopy (EIS) using a PAR 2273 potentiostat/galvanostat (Princeton Applied Research) for frequencies from 1 Hz to 2 MHz [29]. Membranes in the hydroxide form were initially hydrated by immersing in deionized water at room temperature for 24 h before measurement. Samples to be tested (ca. 3 × 1 cm) were clamped into the conductivity cell. This assembly was immersed in deionized water pre-equilibrated to the desired temperature followed by measurement of the conductivity. The water bath was purged with nitrogen so as to avoid forming carbonate ions from absorption of CO_2 from the air. Conductivity measurements were carried out from 25 to 80 °C. The frequency region over which the impedance had a constant value was confirmed. The real component of the impedance at the highest frequency measurement was taken as the effective resistance of the membrane. This was then used to calculate the hydroxide conductivity using Eq. (3).

$$\sigma = \frac{L}{(Z'\mathrm{xA})} \quad (3)$$

where L is the length between sense electrodes (0.425 cm), Z' is the real component of the impedance response at high frequency, and A is the membrane area available for hydroxide conduction.

3. Results and discussion

The synthetic scheme for the preparation of partially fluorinated poly(arylene ether) with pendant quaternary ammonium groups is shown in Fig. 1. The first step is the synthesis of the polymer through a polycondensation reaction. The copolymerization of PHQ and DFBP was carried out in a DMAc/toluene cosolvent in a nitrogen atmosphere at ambient temperature for 20 min followed by reaction at 130 °C for 12 h. Toluene was used to dehydrate the reaction mixture at 130 °C as water was generated during bisphenoxide formation. Second, the chloromethylated polyether (CMPAE) was prepared by Friedel-Crafts electrophilic substitution reaction under anhydrous conditions at 60 °C using PAE as the starting material, 1,1,2,2-tetrachloroethane as the solvent, chloromethyl methyl ether as the chloromethyl reagent, and anhydrous $SnCl_4$ as the catalyst. Extreme reaction conditions, such as high temperature, and excess reaction time could lead to gelation of the polymers due to the formation of methylene bridges between the macromolecular chains. In order to avoid crosslinking and gelation, the chloromethylation reaction was performed at dilute conditions with little catalyst present. Third, the chloromethyl moiety was converted into the quaternary ammonium base by immersing the polymer in an aqueous trimethylamine solution (45%) at room temperature for two days. The QAPAE was dissolved in DMF and cast onto Teflon plates to form ~70 μm thick membranes by evaporating the solvent slowly in the oven at 60 °C. The membrane was tough, ductile and transparent with a faint brown tint. Finally, the membranes were immersed in a 0.1 M sodium hydroxide aqueous solution at room temperature for several times to convert the QAPAE polymer from the chloride form to the hydroxide form.

The chemical structure and composition of the neat PAE and CMPAE were investigated by liquid phase ^{1}H-NMR spectroscopy with $CDCl_3$ as the solvent and reference. As shown in Fig. 2A, the aromatic hydrogens of PAE are divided into two regions: a high-field (6.90–7.20 ppm) and low-field (7.40–7.60 ppm) region. Integration of the peaks in the high and low field regions correspond to 3H: 5H, respectively, reflecting the chemical structure of the PAE repeat units. The ^{1}H-NMR result is consistent with the structure of the PAE copolymer. The high-field NMR response has the characteristic chemical shift for the main-chain ortho-oxygen aromatic protons which reflects shielding from the electron-donating ether linkage. The low-field signals are attributed to the aromatic hydrogens from the strongly electron-withdrawing groups.

The NMR spectrum for the partially chloromethylated PAE (Fig. 2B) is more complex because it includes the uncholorometylated and chloromethylated repeat units. Compared with the

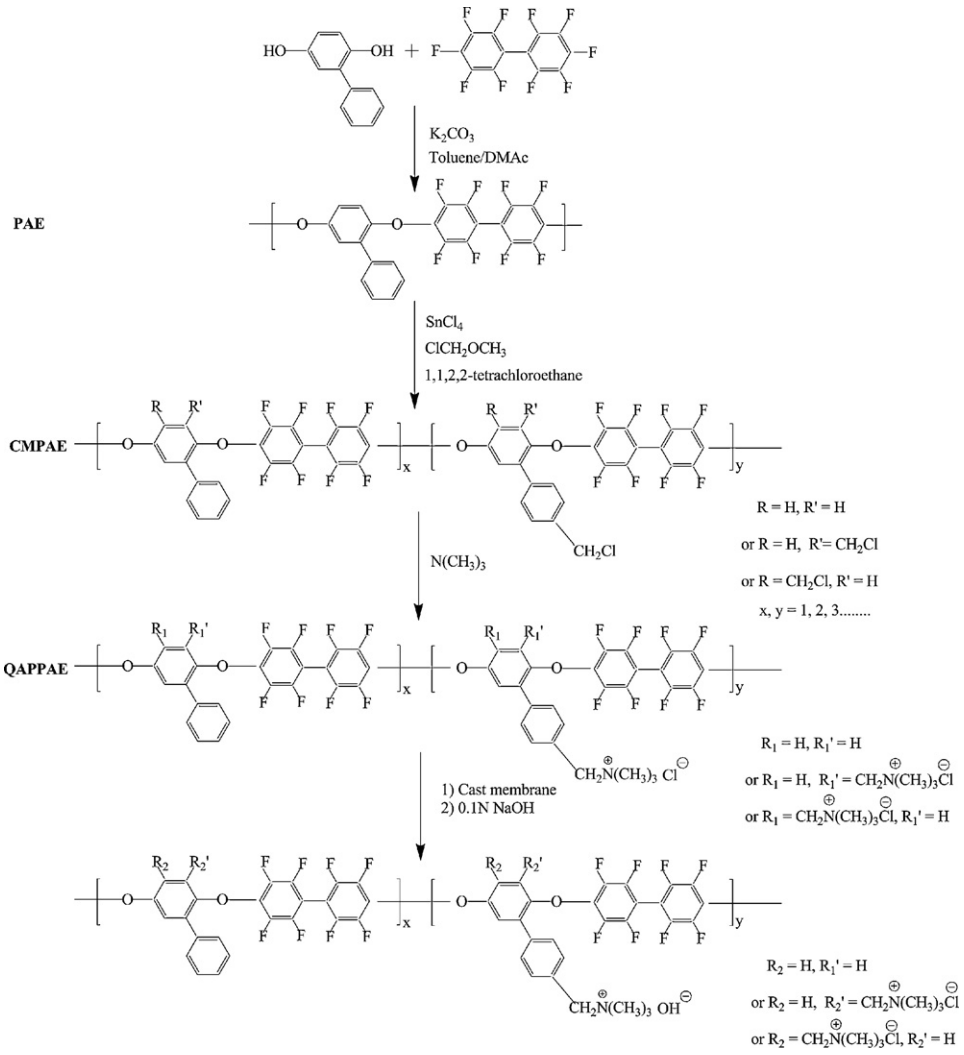

Fig. 1. The synthetic route for partially fluorinated copoly(arylene ether) ionomer with pendant quaternary ammonium groups.

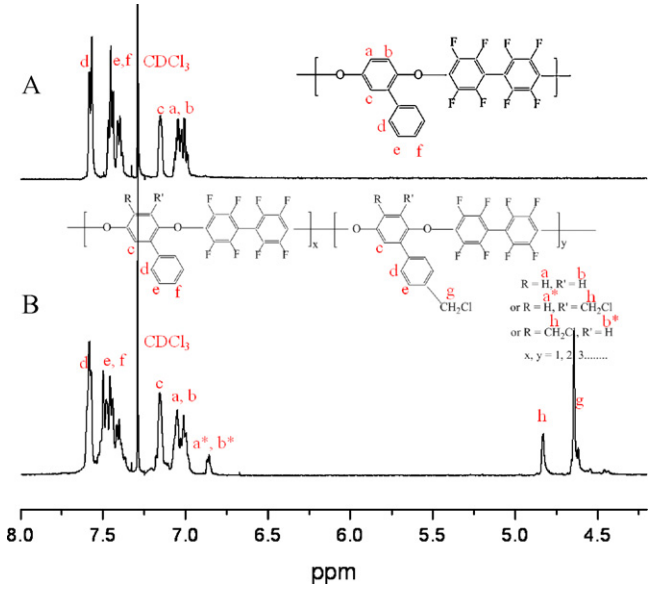

Fig. 2. ^{1}H-NMR of PAE (A) and CMPAE (B) copolymers.

^{1}H-NMR spectrum of PAE in Fig. 2A, the characteristic hydrogen peaks for $-CH_2Cl$ corresponds to the newly formed chloromethyl group, as can be seen at δ = 4.58 (g) and 4.70 (h) in Fig. 2B. The two new peaks for the chloromethyl groups were observed in the NMR spectrum. There are two groups of aromatic rings: those in the backbone and those pendants to the backbone which could be chloromethylaed during the chloromethylation reaction. These new peaks confirm the successful preparation of the chloromethylated copolymer CMPAE.

The degree of choloromethylation (DC), the fraction of chloromethylated repeat units, was determined from the ^{1}H-NMR spectrum of the CMPAE copolymer, by estimating the relative peak area between the aromatic protons and the chloromethyl protons. Since there are 7 aromatic protons, 2 protons at 4.58 and 4.70 ppm in the chloromethylated moiety (Fig. 2B), and 8 protons in the non-chloromethylated moiety, the internal ratio *r*, which is calculated from NMR spectra, as given by Eq. (4) [30].

$$r = \frac{2DC}{7DC + 8(1 - DC)} \tag{4}$$

The calculated DC values from the NMR aromatic and chloromethyl protons are listed in Table 1. The choloromethylation reaction time was from 3 to 12 days with the longer times leading to higher DC values. The DC values obtained ranged from 0.28 to 0.79.

Table 1
Chloromethylation reaction conditions and the degree of chloromethylation (DC).

Polymer	Time (days)	DC[a]
CMPAE-1	3	0.28
CMPAE-2	6	0.49
CMPAE-3	9	0.56
CMPAE-4	12	0.79

[a]Degree of chloromethylation = (number of chloromethyl groups/repeat unit), calculated from ^{1}H-NMR spectra.

The thermal stability of the polymer electrolyte is a key metric for use in fuel cells because they are often operated at high pH and elevated temperatures, between 40 °C and 120 °C. The thermal stability of the polymers synthesized here was studied by use of TGA. The TGA curves for PAE, CMPAE, QAPAE in the chloride form (QAPAE–Cl), and QAPAE in the hydroxide form (QAPAE–OH) are shown in Fig. 3. The 5% weight loss temperature for the neat PAE was ca. 460 °C, as shown in Fig. 3A. PAE is thermally stable because of its rigid aromatic structure. Two decomposition steps were observed in the TGA for CMPAE (Fig. 3B). The first degradation step, from 260 to 320 °C, is attributed to the loss of chloromethyl groups. The second decomposition step, beginning at 410 °C, corresponds to the degradation of the PAE backbone. The TGA curves for QAPAE–Cl and QAPAE–OH are shown in Fig. 3C and D, respectively. The initial weight loss of QAPAE–Cl from 25 to 135 °C is attributed to loss of absorbed water and residual DMF solvent. In addition, it is interesting to note that the dehydration of QAPAE continues well above 100 °C indicating strongly hydrogen bonded water to the amine [17,18]. The second weight loss above 163 °C is due to cleavage of the quaternary ammonium groups from QAPAE–Cl. The loss in mass at temperatures greater than 422 °C is due to degradation of the polymer backbone. As shown in Fig. 3D, it is found that the decomposition temperature of the QAPAE–OH backbone significantly decreased compared to that of QAPAE–Cl. Moreover, the mass loss for the quaternary ammonium groups of the QAPAE–OH occurred at 140 °C. These results show that QAPAE–OH is less stable in the dry, alkaline condition where the activity of hydroxide ions is the highest. This is not the same environment as in a working alkaline fuel cell due to the high state of hydration during operation.

The solubility of the polymers is important in the synthesis, purification, casting as a membrane, and use as an ionomer in forming an electrode. The solubility of PAE, CMPAE and QAPAE was investigated by dissolving 0.03 g polymers in 3 mL of a variety of solvents, as shown in Table 2. It can be seen that PAE and

Table 2
The solubility of PAE, CMPAE and QAPAE in different solvents.

Solvent	PAE	CMPAE	QAPAE
Water	I	I	SW
Ethanol	I	I	SW or S
Methanol	I	I	SW or S
Chloroform	S	S	I
Tetrahydrofuran	S	S	I
N,N-dimethylformamdie	S	S	S
N,N-dimethylacetamide	S	S	S

S: soluble; I: insoluble; SW: swelling.

CMPAE are soluble in polar, aprotic solvents (such as DMF and DMAc) and chloridized solvents (such as chloroform and 1,1,2,2-tetrachloroethane). They are insoluble in some protic solvents such as water, methanol, and ethanol. However, after the addition of the quaternary ammonium groups, QAPAE is soluble or swells in water, methanol and ethanol because of the hydrophilic quaternary ammonium groups. It is noted that the solubility of QAPAE strongly depends on the density of quaternary ammonium groups as represented by the ion exchange capacity or degree of chloromethylation. Excessive chloromethylation should be avoided when the anion exchange polymer is used in a liquid methanol fuel cell.

Water uptake of the ionomers is particularly important during use in an operating fuel cell because swelling effects mechanical integrity of the electrode-membrane structure and conductivity of the membrane itself. Ionomers with inadequate water uptake typically show low ionic conductivity. The water uptake in the ionomers used to fabricate the electrodes has added requirements. Excessive water uptake and swelling within the electrode can result in blockage of the reactant and product gas from the electrodes, obstruction of the catalyst sites resulting in poor catalyst utilization, and mechanical failure within the electrode. The water uptake was measured by measuring the ratio of the mass of water absorbed by the membrane when immersed in water compared to the dry membrane mass. Water uptake is typically a function of the IEC since the quaternary ammonium sites and the counter ion are hydrophilic. The data are summarized in Fig. 4. A clear relationship is observed between higher water uptake and IEC [31]. As the IEC was increased from 0.33 to 1.22 meq g^{-1}, the water uptake increased from 5.45 to 55.02%. It is interesting to see that the water uptake of the QAPAE-3 ionomer was dramatically higher and is related to a percolation threshold [32].

In compassion to a previously reported ionomer (QAPSF) [28], QAPAE-4 shows markedly lower water uptake (Table 3). Here,

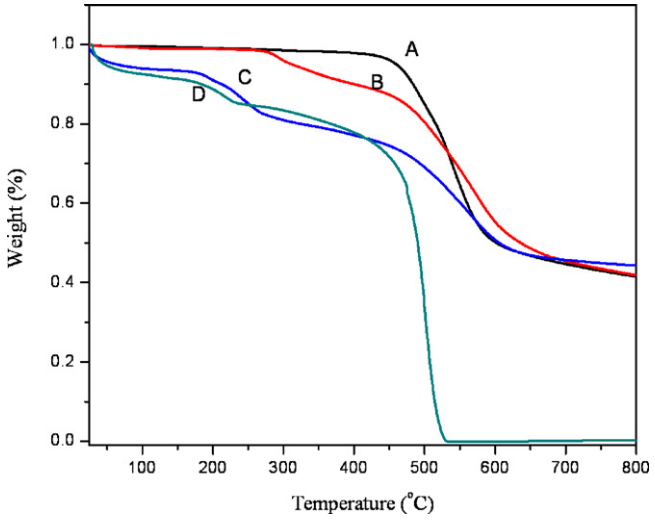

Fig. 3. TGA curves for PAE (A), CMPAE (B), QAPAE–Cl (C) and QAPAE–OH (D).

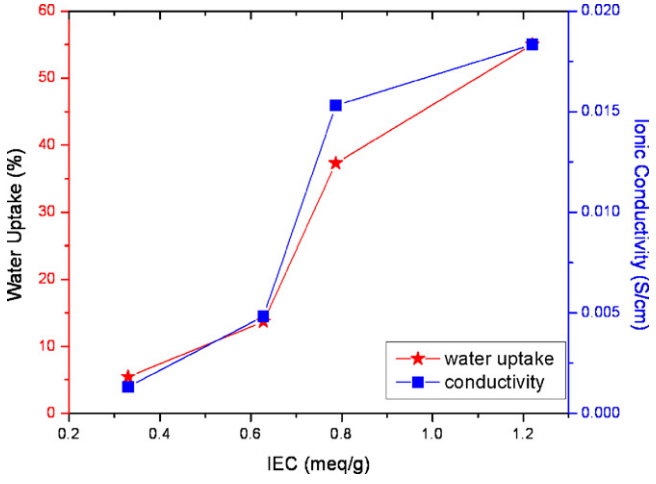

Fig. 4. Water uptake and hydroxide anion conductivity vs. ion exchange capacity.

Table 3
Ion exchange capacity, water uptake, and hydroxide conductivity of QAPAE-4 and QAPSF membranes.

Sample	IEC (meq g^{-1})	Water uptake (%)		Conductivity (mS cm^{-1})	
		25 °C	60 °C	25 °C	60 °C
QAPAE-4	1.22	55.0	75.2	18.3	28.8
QAPSF	1.21	76.6	80.9	21.2	–

QAPAE-4 (IEC = 1.22 meq g^{-1}) had 55.0% water uptake, which is much lower than QAPSF (IEC = 1.21 meq g^{-1}) at 25 °C (76.6%). The low water uptake is due to the presence of the hydrophobic fluorinated biphenyl groups in the polymer backbone, which would also lower the surface tension. As shown in Table 3, QAPAE-4 shows a temperature-dependent water uptake. For example, the water uptake of QAPAE-4 increases from 55.0 to 75.2% when the temperature was increased from 25 to 60 °C.

The ionic conductivity of the polymer electrolyte membrane is critical to fuel cell performance. The ionic conductivity of the membranes was measured by an in-plane method with the membranes in the hydroxide form after being hydrated by immersion in deionized water for 24 h at ambient temperature. The hydroxide conductivity values are shown as a function of the IEC in Fig. 4. The trend in conductivity follows that of water uptake. The highest conductivity, 18.3 mS cm^{-1}, was found for the QAPAE-4 ionomer with an IEC value of 1.22 meq g^{-1}. QAPAE-3 showed moderate conductivity (15.3 mS cm^{-1}). QAPAE-2 and QAPAE-1 had relatively low conductivity, 4.83 and 1.32 mS cm^{-1}, respectively. The ionic conductivity increases rapidly above a critical threshold due to the formation of ion-conducting regions within the polymer [31]. At low IEC values, the conductivity is limited by the ionic connection between domains in the polymer. As the IEC increased, the conductivity increased rapidly as the volume fraction of water and concentration of ionic groups in the membrane increased [33]. As shown in Table 3, QAPSF had a higher conductivity (21.2 mS cm^{-1}) than QAPAE-4 at nearly the same IEC. This is due to higher water uptake of QAPSF compared to QAPAE-4. Water assists in the dissociation of the alkali functionality and facilitated hydroxide transport in the ionomers [31].

Fig. 5 shows the hydroxide conductivity of the partially fluorinated ionomers vs. temperature. In general, the conductivity of all the ionomers increased with temperature due to the higher mobility of hydroxides in the conductive channels within ionomers. For example, the ionic conductivity of QAPAE-4 increased from 18.3 to 38.2 mS cm^{-1} for a temperature rise from 25 to 80 °C. The activation energy for ion-migration, *E*a, was estimated from the linear regression of ln(conductivity) vs. 1000/*T* as shown in Fig. 5, assuming an Arrhenius behavior. The ion transport activation energy, E_a, for the QAPAE ionomers was calculated using Eq. (5).

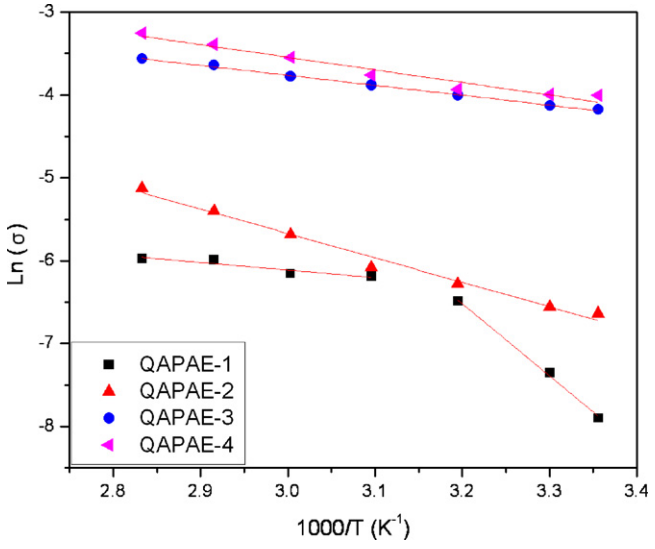

Fig. 5. lnσ vs. 1000/*T* plots for the QAPAE ionomers; the lines show a linear regression.

$$E_a = -b \times R \quad (5)$$

where *b* is the slope of the line regression of lnσ vs. 1000/*T* (K^{-1}) plots, and *R* is the gas constant (8.31 JK^{-1} mol^{-1}).

The E_a for QAPAE which had a high IEC value (0.79 and 1.22 meq g^{-1}) is around 9.97 kJ mol^{-1}. The value is very similar to the E_a of Nafion 117 (9.1 kJ mol^{-1}) and other AEMs (10 to 12 kJ mol^{-1}) [14]. This demonstrates that the hydroxide ion mobility in QAPAE with high IEC is similar to hydrated proton mobility in Nafion 117. However, the *E*a for QAPAE with IEC 0.63 meq g^{-1} has a high value (around 24.53 kJ mol^{-1}) showing that the hydroxide ion mobility in the QAPAE with low IEC is more sensitive to temperature due to the isolated ionic cluster structure. The E_a for QAPAE with IEC 0.33 meq g^{-1} shows two different regions. At low temperature (25–40 °C), the E_a has a high value at 72.37 kJ mol^{-1}; at the elevated temperature (50–80 °C), the *E*a is about 7.62 kJ mol^{-1}.

Fuel cell electrodes were fabricated with the ionomers synthesized here and the performance was evaluated as the cathode of a PEM-based hybrid polymer electrolyte fuel cell. This hybrid fuel cell design enables easy characterization of the AEM electrode and gives insights into the rate limiting processes [27]. In particular, the overall cell performance largely reflects the performance of the AEM cathode because the contributions from other components, e.g. the anode and membrane, are minimal.

Fig. 6 shows the fuel cell performances at 25 °C and 60 °C for the hybrid cell comprising the AEM cathodes made from QAPSF or QAPAE-4 ionomers. The cell was operated with humidified H_2/O_2 streams. The AEM electrode with QAPAE-4 resulted in higher performance than the ones with QAPSF at both 25 °C and 60 °C. The peak power density at 60 °C was 315 mW cm^{-2} for QAPAE-4 and 215 mW cm^{-2} for QAPSF. It is also important to note that the cells did not show any degradation in performance during several days of testing, indicating adequate stability at operating cell conditions.

This improvement in the cell performance is due to the greater degree of hydrophobicity in the catalyst layer created by the QAPAE-4 ionomer. The hydrophobic nature of QAPAE-4 results in lower water uptake compared to QAPSF, see Table 3. The lower water content in the ionomer does lead to lower ionic conductivity because the ionic conduction is nearly proportional to water content, however, ionic conductivity is not the limiting factor in the AEM electrode. Analysis of QAPSF electrodes showed that they had poor performance due to low catalyst utilization [10]. In particular, the high water uptake of the QAPSF electrode inhibited gas transport (reactants transported to the catalyst and products transported away) to the catalyst layer resulting in low active surface area for the catalyst. The loss of active catalytic sites is more pronounced when the cell was operated at higher current density because the rate of water generation is higher. The higher production rate of water causes flooding, which further blocks the catalyst sites. The hydrophobic nature of the fluorinated ionomer, QAPAE-4, decreased the overall water content in the catalyst layer. This leads to faster removal of water produced and provides greater accessibility of the catalyst surface to the gaseous reactants. The performance enhancement with QAPAE-4 ionomer compared to QAPSF is more pronounced at higher current density where the faster removal of water is necessary to maintain sufficient gas transport in the catalyst layer.

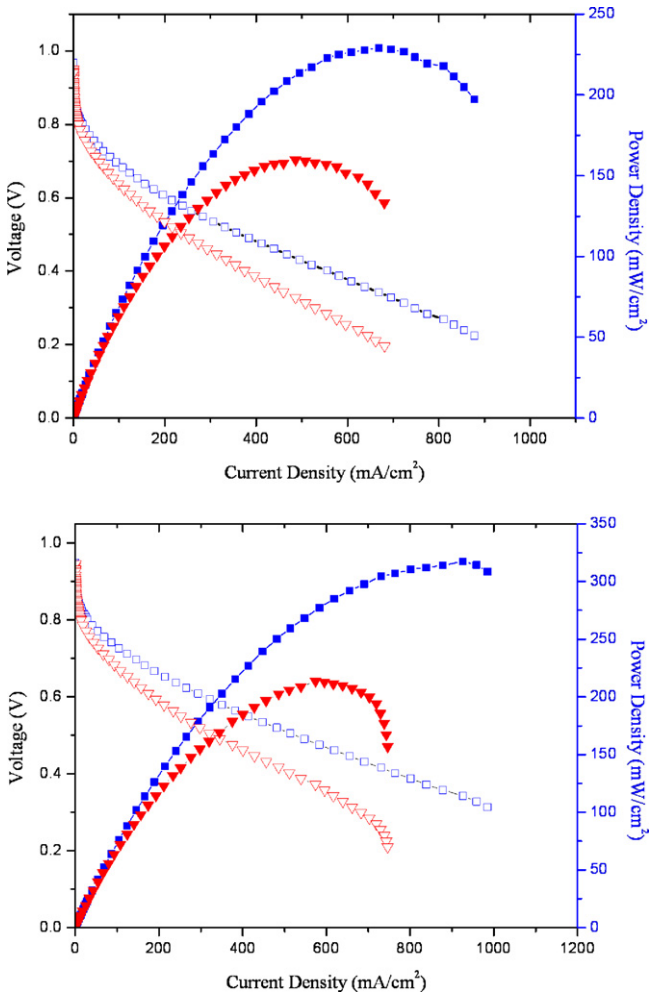

Fig. 6. Cell voltage and power density curves as a function of the current density at 25 °C (top) and 60 °C (bottom) for hybrid fuel cells with the AEM cathodes. The AEM electrodes were made with QAPSF (triangle) or QAPAE-4 (squares). The catalyst loading was 0.5 mg cm^{-1} Pt for all the electrodes. H_2 and O_2 were humidified and supplied at ambient pressure. Solid symbols correspond to power density and open symbols correspond to voltage.

4. Conclusion

A series of novel partially fluorinated poly(arylene ether) copolymers with quaternary ammonium groups were synthesized by polycondensation, chloromethylation, and amination reactions. The IEC of the polymer electrolyte was controlled by adjusting the chloromethylation reaction time. The ionomers also showed good ionic conductivity and low water uptake due to the hydrophobicity of the partially fluorinated backbone. For QAPAE-4, its hydroxide conductivity was 28.8 mS cm^{-1} and water uptake was 75.2% at 60 °C. The AEM electrode fabricated with QAPAE-4 resulted in better performance than ones fabricated with QAPSF. The peak power densities at 60 °C was 315 mW cm^{-2} for QAPAE-4 and 215 mW cm^{-2} for QAPSF. These improvements in the cell performances were attributed to the hydrophobic nature of QAPAE. The properties of the ionomers can be further improved by adjusting the molecular weight of the polymer and optimizing the chloromethylation conditions.

Acknowledgement

The authors gratefully acknowledge financial support from the Army Research Laboratory, contract LCHS22067.

References

[1] W.H. Meyer, Adv. Mater. 10 (1998) 439.
[2] B. Smitha, S. Sridhar, A.A. Khan, J. Membr. Sci. 259 (2005) 10.
[3] G. Wegner, Polym. Adv. Technol. 17 (2006) 705.
[4] J. Spurgeon, M. Walter, J.F. Zhou, P.A. Kohl, N.S. Lewis, Energy Environ. Sci. 4 (2011) 1772.
[5] X. Li, Principles of Fuel Cells, Taylor & Francis, New York, USA, 2005.
[6] Y.S. Kim, B.S. Pivovar, Annu. Rev. Chem. Biomol. Eng. 1 (2010) 123.
[7] M. Rikukawa, K. Sanui, Prog. Polym. Sci. 25 (2000) 1463.
[8] J.R. Varcoe, R.C.T. Slade, Fuel Cells 5 (2005) 187.
[9] M. Ünlü, J. Zhou, P.A. Kohl, Fuel Cells 10 (2010) 54.
[10] M. Ünlü, J.F. Zhou, P.A. Kohl, J. Electrochem. Soc. 157 (2010) B1391.
[11] Y.S. Li, T.S. Zhao, R. Chen, J. Power Sources 196 (2011) 133.
[12] Y.S. Li, T.S. Zhao, J.B. Xu, S.Y. Shen, W.W. Yang, J. Power Sources 196 (2011) 1802.
[13] M.R. Hibbs, C.H. Fujimoto, C.J. Cornelius, Macromolecules 42 (2009) 8316.
[14] M. Tanaka, M. Koike, K. Miyatake, M. Watanabe, Macromolecules 43 (2010) 2657.
[15] Y. Xiong, Q.L. Liu, Q.H. Zeng, J. Power Sources 193 (2009) 541.
[16] J.L. Yan, M.A. Hickner, Macromolecules 43 (2010) 2349.
[17] J.F. Zhou, M. Unlu, I. Anestis-Richard, P.A. Kohl, J. Membr. Sci. 350 (2010) 286.
[18] J.F. Zhou, M. Unlu, J.A. Vega, P.A. Kohl, J. Power Sources 190 (2009) 285.
[19] J. Pan, S.F. Lu, Y. Li, A.B. Huang, L. Zhuang, J.T. Lu, Adv. Funct. Mater. 20 (2010) 312.
[20] J. Fang, P.K. Shen, J. Membr. Sci. 285 (2006) 317.
[21] Y.T. Luo, J.C. Guo, C.S. Wang, D. Chu, J. Power Sources 195 (2010) 3765.
[22] H.K. Xu, J. Fang, M.L. Guo, X.H. Lu, X.L. Wei, S. Tu, J. Membr. Sci. 354 (2010) 206.
[23] T.N. Danks, R.C. Slade, T.J.R. Varcoe, J. Mater. Chem. 12 (2002) 3371.
[24] R.C. Slade, T.J.R. Varcoe, Solid State Ionics 176 (2005) 585.
[25] N. Tzanetakis, J.R. Varcoe, R.C. Slade, T.K. Scott, Desalination 174 (2005) 257.
[26] D.S. Kim, G.P. Robertson, Y.S. Kim, M.D. Guiver, Macromolecules 42 (2009) 957.
[27] M. Ünlü, J.F. Zhou, I. Anestis-Richard, P.A. Kohl, ChemSusChem 3 (2010) 1398.
[28] M. Ünlü, J.F. Zhou, P.A. Kohl, J. Phys. Chem. C 113 (2009) 11416.
[29] N.J. Robertson, H.A. Kostalik, T.J. Clark, P.F. Mutolo, H.D. Abruna, G.W. Coates, J. Am. Chem. Soc. 132 (2010) 3400.
[30] Z. Bai, J.A. Shumaker, M.D. Houtz, P.A. Mirau, T.D. Dang, Polymer 50 (2009) 1463.
[31] J.H. Wang, S.H. Li, S.B. Zhang, Macromolecules 43 (2010) 3890.
[32] D.S. Kim, K.H. Shin, H.B. Park, Y.S. Chung, S.Y. Nam, Y.M. Lee, J. Membr. Sci. 278 (2006) 428.
[33] J.H. Wang, Z. Zhao, F.X. Gong, S.H. Li, S.B. Zhang, Macromolecules 42 (2009) 8711.